NATIONAL ACADEMY OF SCIENCES OF BELARUS

INSTITUTE OF MATHEMATICS

Second International Conference

"FINITE-DIFFERENCE METHODS: THEORY AND APPLICATION"

(CFDM98)

PROCEEDINGS

Volume 3

EDITED BY
A.A.SAMARSKII

Minsk, Belarus

SOFTWARE FOR MATHEMATICAL MODELING IN THE PROBLEMS OF LASER-PLASMA TREATMENT OF MATERIALS

VLADIMIR I. MAZHUKIN
VADIM V. NOSOV
SERGEY.G.GORBACHENKO
Institute of Mathematical Modelling, RAS
4a Miusskaya Sq., 125047 Moscow, Russia

VALERY I. SHCHEGLIK

Institute of Mathematics, NASB
11 Surganov St., 220072 Minsk, Belarus

Mathematical modelling in the field of laser-plasma treatment of materials presents an enhanced complexity problem and involves consideration of a large number of interrelated processes with nonlinear evolution characteristics. Therefore automatization of computations and result processing become an important problem, which can be effectively solved by means of specially developed software. The paper presents two products that illustrate this approach. The LPT-2D software is developed for self-consistent modelling of heating and evaporation of a metal target and dynamics of laser plasma in 2D axis-symmetrical formulation. The LScan-3D software is intended for computations of 3D thermal effects, induced by moving laser beams in an irradiated slab. Both software run in WIN32 envieronment, have a convinient user interface, graphical presentation subsystem, data and results collecting capabilities.

1. Introduction

At present, technologies based on the effect of laser radiation on condensed media are successfully applied in very different fields of human activities, including metallurgy, microelectronics, medicine, and basic scientific researches. The wide application is explained primarily by unique properties of laser beam as an energy source. In recent years there is a tendency to use high power and ultra-short laser pulses of nanosecond and picosecond duration. In this time range it becomes extremely difficult to derive any information on occurring processes, to solve problems of diagnostics, control and optimization.

Laser action on a target is accompanied by a variety of physical phenomena, which are described by nonlinear equations of mathematical physics and are highly complicated for theoretical analysis [1]. Among the phenomena there are: the processes of heating of a target with volumetric or surface energy release, target cooling and generation of thermal stresses; phase transitions: melting, solidification, evaporation; gas-dynamic expansion of evaporated matter; optical breakdown, plasma formation, and linear and continuous radiation transfer. In this situation mathematical modelling becomes a very important method of investigation, and can be applied either as an autonomus approach or simulteneously with experimental studies. In the later case the experimental data surve as an a'priory information, support adjustment of mathematical models and interpretation of results.

Modelling of phenomena under laser treatment is based on ***hierarchy of mathematical models***. In doing so, physical aspects of the phenomena are studied on more complex and (in most cases) one-dimensional models, whereas engineering aspects are treated on more simple 2D and 3D models that are solved in more complex configurations. The complex configuration term means complex geometry of the domain considered or (as in our case) complex set of input parameters.

Automatization of scientific computations presents a very important aspect of studies. In the paper two software products will be considered developed by the present authors. LPT-2D software is developed for self-consistent modelling of heating and evaporation of a metal target and dynamics of laser plasma in

2D axis-symmetrical formulation, and is related in particular to the problems of Pulsed Laser Deposition and Laser-Plasma Shock Processing. LScan-3D software is intended for computations of 3D thermal fields, induced by moving laser beams in an irradiated slab, and permits one to predict the size of a heat-affected zone, heating and cooling rates, and to estimate laser-induced thermal stresses resulted.

2. Laser-Plasma Treatment problems – LPT-2D software

2.1. *Mathematical model*

Let us consider a solid target placed into a cold gaseous medium initially transparent for laser radiation which propagates along the normal to the target surface. If the intensity of the laser radiation is high enough, then the temperature of the matter becomes higher than the normal boiling temperature already at the onset of the laser pulse. An intensive evaporation process starts and a thin hot gaseous layer is formed adjacent to the target surface. One fraction of the laser energy is absorbed by the hot layer and the other by the target surface. Between the condensed and gaseous media a transient area appears referred to as the Knudsen layer. The Knudsen layer is usually considered as a gas-dynamic gap, the parameters of which are determined from the external side with some assumptions on a nonequilibrium distribution function inside the layer.

Laser plasma, emerging near the target in the evaporated substance or environmental gas, is characterised by strong spatial variation of density ρ and temperature T resulted from appreciable hydrodynamic phenomena. Therefore in most cases the laser plasma has a variable optical thickness, and reabsorbtion and radiation transfer processes become important, if the geometrical sizes of the plasma cloud are large enough. The plasma of variable optical density is most complicated for investigation. Two different phenomena: hydrodynamic expansion (compression) and radiation transfer contribute comparably to the energy balance of the system. Mathematical description of these phenomena in plasma is usually performed by means of the Radiative Gas Dynamics (RGD) model [2-5].

The model is based on the following assumptions:

i) condensed medium heating and evaporation processes are described in the framework of one phase version of Stefan problem [6];

ii) plasma is considered to be an absorbing medium (excluding elastic scattering);

iii) plasma is described in nonviscous non-heat-conductive gas approximation;

iv) Local Thermodynamic Equilibrium (LTE) conditions are fulfilled at all the points of the plasma domain.

Consider the (r, z) cylindrical coordinate system (axial symmetry case) moving with the velocity V_{lv} of the evaporation front along the z-axis. Under the above assumptions the problem can be formulated as follows.

The condensed medium is described by the nonlinear heat transfer equation:

$$\frac{\partial(\rho_s C_p(T_s)T_s)}{\partial t} - V_{lv}\frac{\partial(\rho_s C_p(T_s)T_s)}{\partial z} = \frac{1}{r}\frac{\partial}{\partial r}\left(r\lambda(T_s)\frac{\partial T_s}{\partial r}\right) + \frac{\partial}{\partial z}\left(\lambda(T_s)\frac{\partial T_s}{\partial z}\right), \quad (1)$$

$$0 < r < L_r, \qquad 0 < z < Z_0,$$

where $C_p, \lambda, \rho_s, T_s$ are the specific heat, thermal conductivity, density, and the temperature of the target, respectively. The processes in the gaseous medium are described by the unsteady RGD equation system. The governing equations are:

$$\frac{\partial\rho}{\partial t} + \frac{1}{r}\frac{\partial}{\partial r}(r\rho u) + \frac{\partial}{\partial z}(r(v - V_{lv})) = 0, \quad (2)$$

$$\frac{\partial\rho u}{\partial t} + \frac{1}{r}\frac{\partial}{\partial r}(r\rho u^2) + \frac{\partial}{\partial z}(ru(v - V_{lv})) = -\frac{\partial(p+\omega)}{\partial r}, \quad (3)$$

$$\frac{\partial\rho v}{\partial t} + \frac{1}{r}\frac{\partial}{\partial r}(r\rho u(v - V_{lv})) + \frac{\partial}{\partial z}(r(v - V_{lv})^2) = -\frac{\partial(p+\omega)}{\partial z}, \quad (4)$$

$$\frac{\partial\rho\epsilon}{\partial t} + \frac{1}{r}\frac{\partial}{\partial r}(r\rho u\epsilon) + \frac{\partial}{\partial z}(r\rho(v - V_{lv})\epsilon) = -\left[\frac{1}{r}\frac{\partial(ru)}{\partial r}\right] - \frac{1}{r}\frac{\partial W_r}{\partial r} - \frac{\partial W_z}{\partial z} - \frac{\partial G}{\partial z}, \quad (5)$$

$$p = p(\rho, T), \epsilon = \epsilon(\rho, T), \quad (6)$$

$$\vec{\Omega}\ \mathrm{grad}\, I_\nu + \kappa_\nu I_\nu = \kappa_\nu I_{eq}, \tag{7}$$

$$\vec{W} = \int_0^\infty d\nu \int \vec{\Omega} I_\nu d\Omega, \qquad \kappa_\nu = \kappa_\nu(\nu, \rho, T), \tag{8}$$

$$\frac{\partial G^+}{\partial z} + \kappa_l G^+ = 0, \qquad \frac{\partial G^-}{\partial z} - \kappa_l G^- = 0, \qquad G = G^+ + G^-, \tag{9}$$

$$0 < r < L_r, \qquad Z_0 < z < L_z,$$

where u, v are the flow velocity components along the r-axis and z-axis; $W_r, W_z, \vec{W}$ are the full radiation flux and its components; ϵ and p are the internal energy and pressure of the plasma; κ_l is the absorption of the laser radiation; G, G^+, G_- are the full intensity of laser radiation and intensities of forward-directed and reflected waves of the laser radiation, respectively; κ_ν, I_ν denote the spectral absorption and spectral intensity of plasma radiation; $\nu, \vec{\Omega}$ are the frequency and direction of a photon. In the system of equations (2) is the continuity equation, (3),(4) are the momentum transfer equations along the r-axis and z-axis, (5) is the internal energy balance, (6) are the equations of state, (7) is the radiation transfer equation, (8) is the radiative flow equation, (9) is the transfer equation for laser radiation.

The charge composition of plasma is described by the nonlinear system of equations of Saha [2,7]:

$$\frac{N_e \sum_{m=0}^{M^{z+1}} N_m^{z+1}}{\sum_{m=0}^{M^z} N_m^z} = \frac{g_e g^{z+1}}{g^z}\left(\frac{mT}{2\pi\hbar^2}\right)^{3/2} exp(-J^z/T), \qquad z = 0, 1, ..., Z_{max}. \tag{10}$$

Here N_e, N_m^z denote the number density for electrons and ions, g_e, g^z are the statical weights, J^z is the ionization potential, $m, \hbar$ refer to the mass of an electron and reduced Planck constant.
The absorption coefficient of laser radiation κ_l is determined as [2,7]:

$$\kappa_l = \frac{8\pi e^6}{3mhc(6\pi mk)^{1/2}} \frac{N_e \sum z^2 N^z}{\nu^3 T^{1/2}} \left(1 - exp(-h\nu/kT)\right), \tag{11}$$

where e is the charge of an electron, z is the charge of an ion, k is the Boltzmann constant.

The system of equations (2)-(11) is supplemented with boundary conditions. On the $z = Z_0$ interface between the condensed and gaseous media the conditions are formulated which present three conservation laws and two additional relations. The key parameter of these relations is the Mach number which can be equal to 1 (that corresponds to evaporation into the medium with a neglegable pressure) or less then 1. In the later case the processes in condensed and gaseous media become interrelated and should be considered as a unified problem:

$$\begin{array}{ll} z = Z_0: & \lambda(T_s)\frac{\partial T_s}{\partial z} = G_s + W_z - L_v \rho_s V_{lv}, \\ & G_s = (1 - R(T_s))G^+, \quad G^- = (1 + R(T_s))G^+, \quad W_z = cU/2, \\ & \rho_s V_{lv} = \rho(v - V_{lv}), \quad p_s + \rho_s V_{lv}^2 = p + \rho(v - V_{lv})^2, \\ & T = T(T_s, M), \quad \rho = \rho(T_s, M), \end{array} \tag{12}$$

where L_v is the latent heat of evaporation, R, U denote the target surface reflectivity and desnity of plasma radiation. The boundary conditions for the condensed medium are:

$$\begin{array}{ll} z = 0: & \lambda(T_s)\frac{\partial T_s}{\partial z} = 0, \\ r = 0: & \lambda(T_s)\frac{\partial T_s}{\partial r} = 0, \\ r = L_r: & \lambda(T_s)\frac{\partial T_s}{\partial r} = 0. \end{array} \tag{13}$$

The boundary conditions for the gaseous medium are :

$$\begin{array}{ll} z = L_z: & p = p_0, \quad W_z = -cU/2, \\ r = 0: & v = 0, \quad W_r = 0, \\ r = L_r: & p = p_0, \quad W_r = -cU/2. \end{array} \tag{14}$$

At the initial time moment $t = t_0$, the temperature of both target and environment gas is set to be T_0, and the gas pressure is p_0.

The spectral absorption $\kappa(\nu, \rho, T)$, as well as the equations of state $p(\rho, T)$ and $\varepsilon(\rho, T)$ are evaluated in advance for the predefined ranges of T and r. The evaluation is based on the solution of self-adjusted field equations (method of Hartree-Fock-Sletter). For subsequent application in a multigroup procedure for continuous radiation transfer, the values obtained are averaged within each group using the Plank method. The calculation results are then saved in three-dimensional tables for $\kappa_k(\nu, \rho_i, T_n)$ and two-dimensional for $p_k(\rho_i, T_n)$, $\varepsilon_k(\rho_i, T_n)$. The i, n, k indices refer to the rows, columns and layers (groups) of tabulated values.

2.2. *The solution algorithm*

Solution algorithm is based to a large extent on the approach [3] for the problems of the dynamics of emitting gas. The overall computation scheme for solving the system of RGD equations and heat transfer equation in the condensed medium at each time step $t = t^j$ can be presented as a combination of several stages.

In the first stage the equations of multigroup diffusion are averaged on a difference level with respect to photon energies, based on the gas-dynamic values and the temperature as obtained from the previous t^{j-1} layer. Averaging is produced by means of the solution of N_k elliptic-type equations. For the reduction of the computational time, the coefficients of the thus-obtained averaged equation were considered "frozen" during the J time step. Therefore the averaging procedure was executed once in every J time steps rather than in every step. On the second stage the diffusion equation and the equation for energy transfer are solved together. In the third the gas-dynamics equations are solved. For finite-difference approximation FLIC method is used [8]. The characteristic feature of this method is the Euler-Lagrange approach.

While all the quantities in the gaseous phase are determined they are utilised to resolve boundary conditions for the one-phase version of the Stefan problem in the condensed medium: to determine the Mach number and total energy flux (laser + plasma radiation) values on the interface. Further the fourth stage is executed, finite-difference equations of heat transfer are solved by the alternating directions method [9] and all the 4 stages are cyclically repeated to reach convergence.

2.3. *The modelling results*

The LPT-2D software allows one to model evolution of gaseous-plasma medium in non-self-consistent formulation, separately for heating and evaporation of the target.

In the computational experiment presented the laser action on the metal target in air and Al vapour environment is considered. The ambient pressure of both media is set to be 1Bar. The initial temperatures of the air and Al vapour are equal to 300K and 0.2eV, respectively, which approximately match the evaporation temperatures on the outer side of the Knudsen layer under normal conditions. The initial densities are equal to $\rho_{air} = 1.25 \times 10^{-3} g/cm^3$, $\rho_{Al} = 1.4 \times 10^{-4} g/cm^3$. The initial region of optical breakdown is treated as a thin layer of hot plasma ($\Delta z = 5 \times 10^{-3} cm, \Delta r = 2.4 \times R_f, T_0 = 1eV$) placed along the irradiated surface of the target. The temporal-spatial distribution of laser pulse intensity is chosen to be the product of two Gaussians:

$$G = G_0 exp(-r^2/R_f^2) exp(-t^2/\tau^2)$$

with the following parameters $G_0 = 5 \times 10^9 W/cm^2$, $\tau = 10^{-8} s$, $R_f = 0.25cm$.

The mathematical modeling have permitted us to reveal the peculiarities of laser plasma development under the action of ultrashort laser pulses. In general, there are three mechanisms of energy dissipation and transfer in laser plasma evolution, namely, ionization of a gaseous medium, work of compression forces and transfer of plasma intrinsic radiation. The characteristic feature of ultrashort action is that the ionization mechanism dominates over all the period of laser action. This results in fast propagation of the ionization wave toward the radiation source and fast heating of the gaseous medium without appreciable gas-dynamic effects being observed. Depicted in Figs. 1-4 are a 2D spatial distribution of the temperature T and density ρ at the onset of laser pulse $t = -4.9ns$ (Figs. 1,2) and after the pulse termination $t = 30ns$ (Figs. 3,4). The temperature of the hot region achieves the maximum $T_{max} = 6.5eV$. However, variation of gas-dynamic and radiative components is insignificant, which is observed on the density plot of Fig. 2. The maximum pressure of the hot region reaches approximately 1.5kBar, which leads to the onset of gas-dynamic expansion. At the time $t = 30ns$ the density of the hot region falls down approximately by one order of magnitude, Fig. 4. The size of disturbed region along the z-axis ($\Delta z \approx 0.6cm$) becomes comparable to the initial size of the hot region.

One of the important characteristics of the process is energy flux value, reaching the surface of the target and the ratio of two components of the flux. Presented in Fig. 5 are the temporal plots of laser radiation fluxes G_s and plasma radiation fluxes W_s at the target surface.

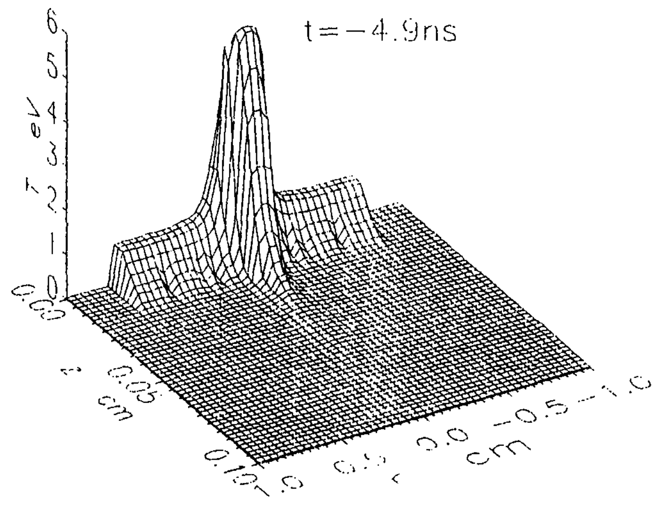

Fig. 1. 2D spatial distribution of temperature T at $t = -4.9ns$ for the air plasma.

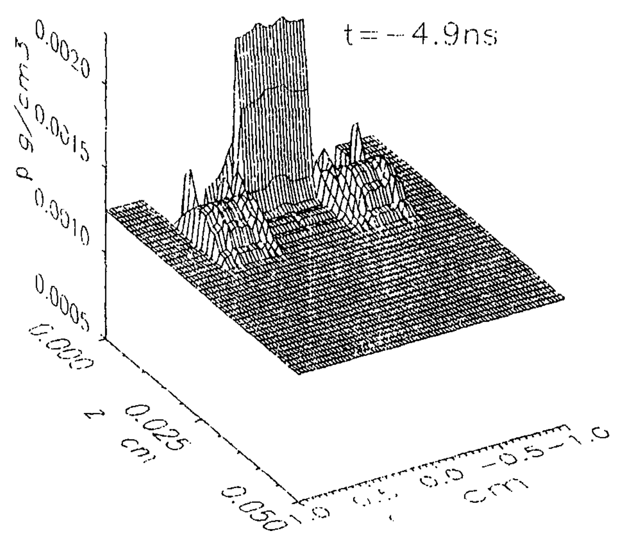

Fig. 2. 2D spatial distribution of density ρ at $t = -4.9ns$ for the air plasma.

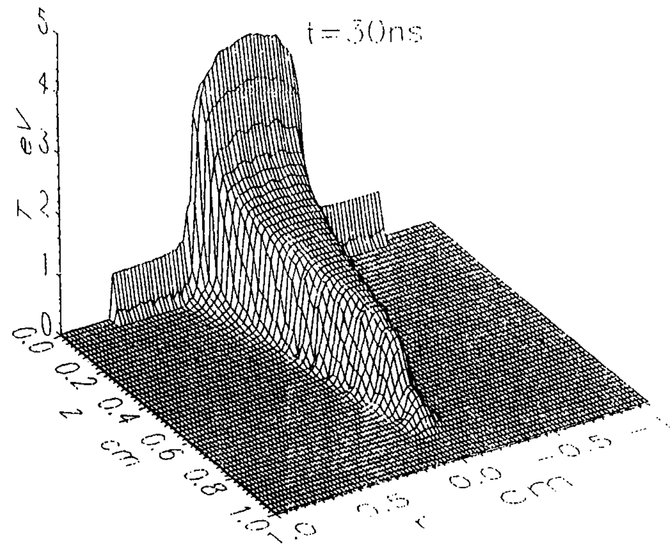

Fig. 3. 2D spatial distribution of temperature T at $t = 30ns$ for the air plasma.

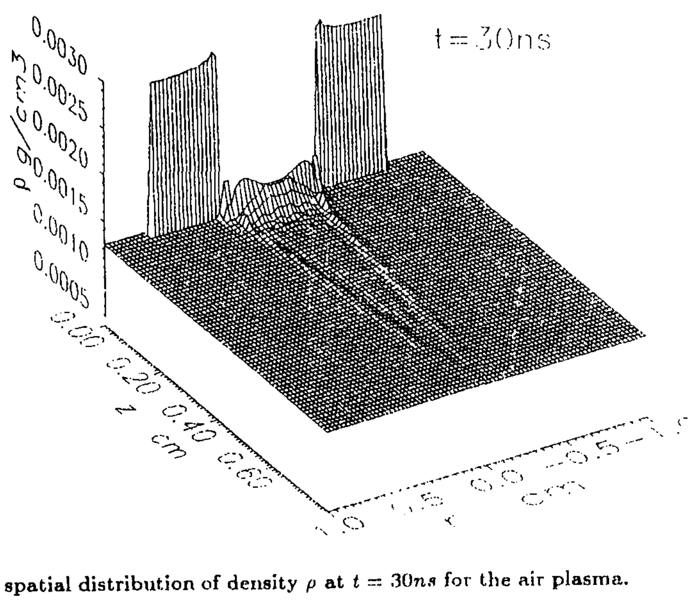

Fig. 4. 2D spatial distribution of density ρ at $t = 30ns$ for the air plasma.

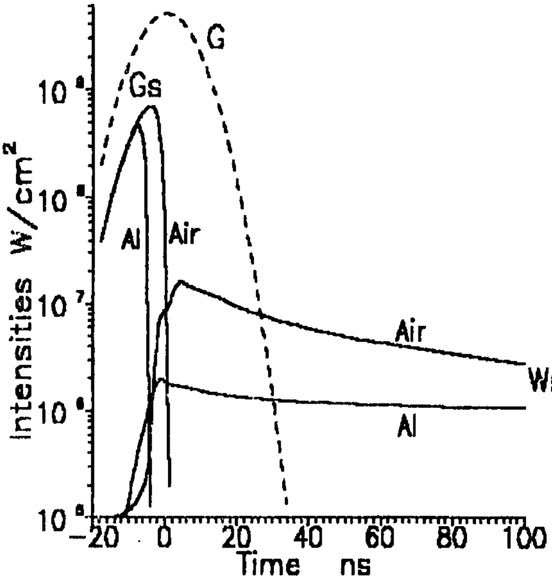

Fig. 5. Time dependencies of laser radiation flux on the target surface Gs(t), plasma radiation flux Ws(t) and intensity of incident laser radiation G(t) for the air and Al vapour plasma.

3. Laser thermohardening problems - LScan-3D software

Laser heating of solids without melting and evaporation of an irradiated surface is generally referred to as thermal treatment [1,10-12]. Its main objective is to change the microhardness and wear resistance of material. As compared to laser-plasma treatment, this approach is characterized by a more simple set of physical processes. However, the dimensionality of the problems to be considered increases, because in most cases the thermohardening is performed by a moving laser beam and, consequently, the heat transfer equation becomes three-dimensional. Therefore peculiarities of the process dynamics should be better studied by means of specialized software, maximally adjusted to all the features of particular problems.

3.1. *Mathematical model*

Let us consider the problem of laser heating of a solid slab irradiated by a normally incident laser beam. A rectangular coordinate system is introduced with the XY coordinate plane on the top surface of the slab and the z-axis directed along the internal normal to this surface. In this coordinate system heat and radiation transfer equations take the form:

$$\rho C_p(T)\frac{T}{t} = \operatorname{div}\lambda(T)\operatorname{grad}T - \frac{\partial G}{\partial z}, \quad \frac{\partial G}{\partial z} + \kappa G = 0, \tag{18}$$
$$0 < x < l_1, \quad 0 < y < l_2, \quad 0 < z < l_3,$$

where κ denotes the absorption coefficient and other notations are the same as for the LPT model considered above.

The sides and bottom of the slab are assumed to be impermeable to heat:

$$\lambda(T)\operatorname{grad}T = 0. \tag{19}$$

On the focal plane $z = 0$ the following conditions are used:

$$\lambda(T)\operatorname{grad}T + \sigma T^4 = 0, \quad G = (1 - R(T))G_{sur}, \quad G_{sur} = \sum G_i, \tag{20}$$
$$G_i = G_0 G_s(x - v_x t, y - v_y t, r_f)G_t(t, \tau_l),$$

where σ is the black body radiation constant, G_0 denotes the peak intensity, G_s, G_t describe spatial and temporal intensity distribution in the focal plane.

Let us consider some features of the model. First of all, the nonlinearity of the model should be mentioned resulting from temperature dependence of heat conductivity, specific heat and absorptivity. In the case of metal, temperature variation from the room temperatute to the melting point causes specific heat to change by 10-20%, while thermal conductivity can become 2-3 times lower and absorptivity can increase 2-8 times. Therefore these factors should be necessarily taken into account to predict the temperature distribution correctly.

The σT^4 term in the boundary conditions describes energy removal from the surface by equilibrium black body radiation. This quantity presents one of the most important diagnostic indicator of the process.

A laser beam is characterised by the following parameters: peak intensity G_0, pulse duration τ_l and pulses repetition frequency f, focal radius r_f, intensity distribution in space (rectangle, Gaussian) and time (rectangle, triangle, Gaussian). Beam movement is specified by setting its initial position, two components of scanning velocity, and scanning area (rectangle) sizes and position. The system is also capable to simulate continuous treatment when the intensity value is kept constant under the entire time period.

An interesting feature of the laser system specification is that it is possible to set several moving sources, which act simulteneously in their own scanning areas. This configuration relates to modelling of the so-called combined influence. Example of possible scanning areas configuration and scanning beam trajectories are presented in Fig. 6.

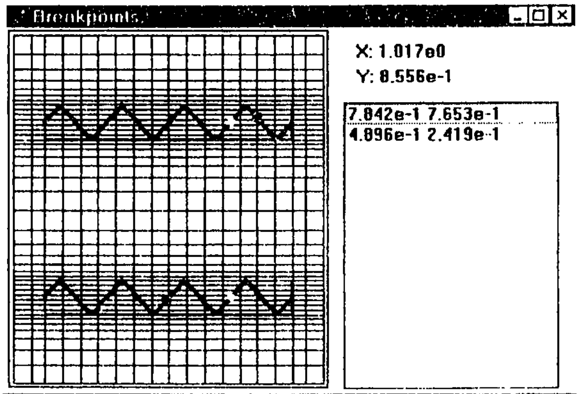

Fig. 6. Topo-plot of temperature plot at t=0.8s and z=0.

The problem formulation presented above relates to the case of volumetric energy release. Physically it means, that the depth of the skin layer (radiation penetration depth) is comparable to or greater than the typical spatial size of the problem. In the opposite case, the radiation transfer equation is excluded from consideration, and the boundary condition at $z = 0$ takes the form

$$\lambda(T)\mathrm{grad}T + \sigma T^4 = (1 - R(T))G_{sur}. \tag{21}$$

At the initial time moment the temperature distribution is uniform, $T = T_0$.

3.2. *Computational grid and algorithm of solution*

Construction of computational grid in multi-dimensional problems presents a subject of special importance. In the case considered the specific features of the differential problem impose the following conditions: (i) the grid in the XY plane should be fine enough in every scanning area; (ii) in the z direction the grid nodes should concentrate toward the irradiated surface which is necessary to track precisely the temporal profile especially in the case of volumetric energy release. Example of computational grid (XY cross-sections) is presented in Fig. 7.

The heat transfer equations have been approximated by the weighted two-layer finite-difference scheme ($\sigma = 0.5$ or $\sigma = 1$) deduced by the integro-interpolation method [9] and symmetric scheme for radiation transfer equation have been applied.

The algorithm for integration of the unsteady-state boundary problem has been based on several enclosed cycles. In the most outer cycle subsequent time steps are performed. Each transition from t^j to t^{j+1} time layer requires nonlinear algebraic equation system to be solved and is performed by two enclosed cycles.

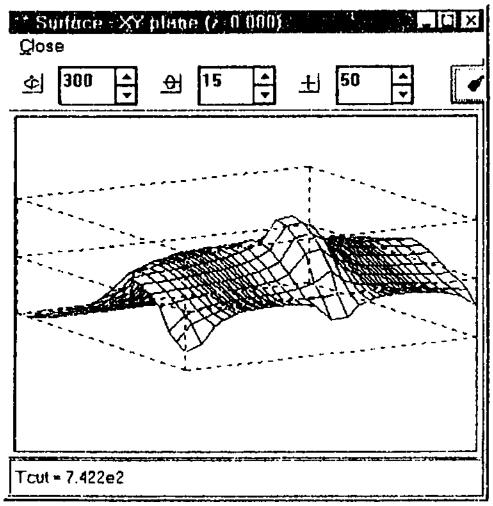

Fig. 8. Topo-plot of temperature plot at $t = 0.8s$ and $z = 0$.

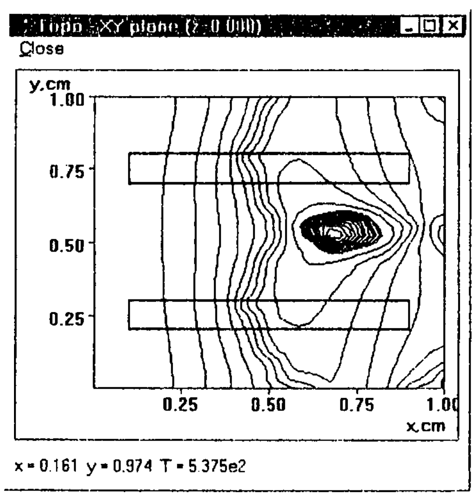

Fig. 9. Topo-plot of temperature plot at $t = 0.8s$ and $z = 0$.

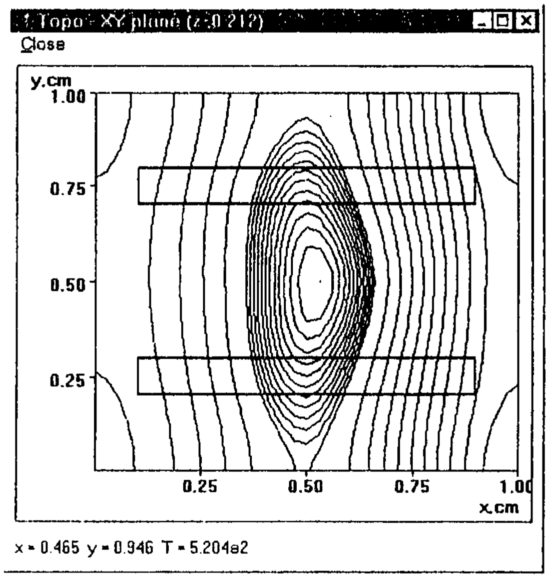

Fig. 10. Topo-plot of temperature plot at $t = 0.8s$ and $z = 0.212$

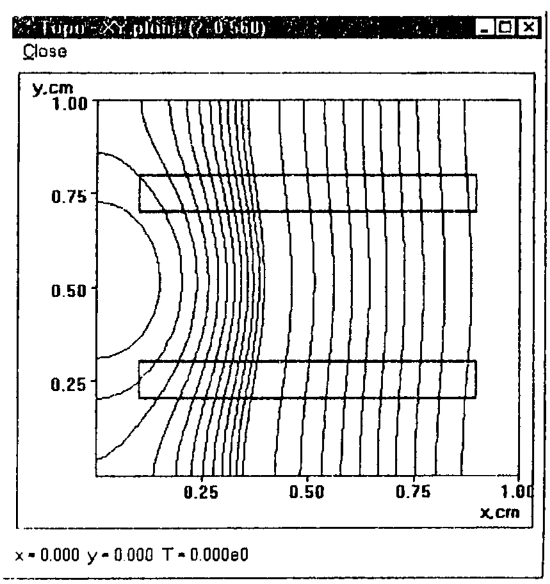

Fig. 11. Topo-plot of temperature plot at $t = 0.8s$ and $z = 0.55$

tations that differ by sets of input parameters, analysis and comparison of predicted results. This procedure in many cases becomes iterative, when the direction of further steps of the experiment is determined on the basis of analysis of the already obtained results. Due to the above features of the investigation procedure, the computational experimental supported software should provide convinient tools for input data preparation, computations execution, results analysis, as well as collecting and systematization of all this information. These objectives are appeared to be achieved easier if the software is developed by means of object-oriented programming and is based on ***variant*** or ***document*** notion (according to Microsoft Foundation Classes terminology). This object includes all the necessary data structures for input parameters and modelling results, each of them can be updated by particular data specific operations, but all the set of data (the document) has its unique name and can be treated as a whole.

Other important feature of modelling software is the so-called export capabilities that make it possible to convert the data of a document from internal to some standard (for example ASCII) format for further processing by means of external software. Frequently, this operations becomes necessary on a final stage of research when the results obtained should be organized and presented on publication quality figures.

5. Conclusion

The paper presents two products, intended for automatization of computations in the filed of modelling for laser treatment of materials. The LPT-2D software realizes the self-consistent model of heating and evaporation of a metal target and dynamics of laser plasma in 2D axis-symmetrical formulation. The LScan-3D software is intended for computations of 3D thermal effects, induced by moving laser beams in an irradiated slab.

Acknowledgment

The studies presented have been performed under the support from FRRF (Grant No. 97-01-00942).

References

[1] V. I. Mazhukin, A. A. Samarskii, *Mathematical modeling in the Technology of Laser Treatment of Material. Review.*, Surveys on Mathematics for Industry, 4 (1994), pp. 85--149.
[2] Ya. B. Zeldovich, Yu. P. Raizer, **Physics of shock waves and high-temperature hydrodynamic phenomena** (Nauka, 1966) (in Russian).
[3] B. N. Chetverushkin, **Mathematical modeling for dynamics of radiating gas** (Nauka, 1985) (in Russian).
[4] V. I. Mazhukin, I. Smurov, G. Flamant, *2D-simulation of the system: laser beam + laser plasma + target*, Applied Surface Science. **86** (1996), pp. 303-309.
[5] V. I. Mazhukin, I. Smurov, G. Flamant, *Simulation of laser plasma dynamics: influence of ambient pressure and intensity of laser radiation*, J. Comp. Phys. **112** (1994), pp. 78--90.
[6] H. S. Carslaw, J. G. Jaeger, **Conduction of heat in solids** (Clarendon, Oxford, 1959).
[7] M. Venugopalan (Ed.), **Reactions under plasma conditions.I** (Wiley-Interscience, 1970).
[8] R. A. Jentry, R. E. Martin, B. A. Daly, J. Computational Physics. **6** (1966), p. 87.
[9] A. A. Samarskii, **Theory of difference schemes** (Nauka, 1989) (in Russian).
[10] N. N. Rykalin, A. A. Uglov, I. V. Zuev, A. N. Kokora, **Laser and electron-beam treatment of materials** (Mashinostrojenije, 1985) (in Russian).
[11] **European Scientific Laser Workshop on Mathematical Simulation** (Lisbon, 1989) pp. 73--142.
[12] N. G. Basov (Ed.), *Laser Technology and investigation automation*, Proc. Lebedev Inst. **198** (1989), pp. 5-23.
[13] A. A. Samarskii, A. V. Gulin, **Numerical Methods** (Nauka, 1989) (in Russian).